

# Consecutive acoustic observations of an Atlantic herring school in the Northwest Atlantic

Thomas C. Weber, Héctor Peña, and J. Michael Jech

Weber, T. C., Peña, H., and Jech, J. M. 2009. Consecutive acoustic observations of an Atlantic herring school in the Northwest Atlantic. – ICES Journal of Marine Science, 66: 1270–1277.

Several successive images of the same school of Atlantic herring (*Clupea harengus*) were collected over the course of  $\sim 1$  h just north of Georges Bank in the Northwest Atlantic. Although the fish may not have been in their natural, undisturbed state, we observed what appeared to be the fish school fragmenting and dispersing, using a split-beam and a multibeam echosounder. Calibrated, 38 kHz, split-beam echosounder (Simrad EK60) and trawl-catch data provided accurate measures of the fish density beneath the vessel. Uncalibrated, 400 kHz, multibeam-echosounder (Reson 7125) data provided synoptic observations of the fish school including estimates of the school volume, morphology, and behaviour. Observations of the angular dependence in the multibeam-echosounder measurements of backscatter from fish allow investigation of the efficacy of extrapolating fish-school densities measured by the split-beam echosounder to the entire school.

**Keywords:** Atlantic herring, fish schools, multibeam echosounder, split-beam echosounder.

Received 6 August 2008; accepted 6 December 2008; advance access publication 9 April 2009.

T. C. Weber: Center for Coastal and Ocean Mapping, University of New Hampshire, Durham, NH, USA. H. Peña: Institute of Marine Research, PO Box 1870 Nordnes, N-5817 Bergen, Norway. J. M. Jech: Northeast Fisheries Science Center, 166 Water Street, Woods Hole, MA, USA. Correspondence to T. C. Weber: tel: +1 603 8621659; fax: +1 603 8620839; e-mail: weber@cocom.unh.edu.

## Introduction

Single-beam echosounders, often with split-beam transducers, are commonly used for estimates of fish biomass, investigations of aggregation morphology, and species classification (Simmonds and MacLennan, 2005). These measurements are inherently two-dimensional, sampling in depth and time if left in a fixed location, or depth and range if moving. Depending on the spatio-temporal structure of the fish, this sampling approach can result in spatial aliasing. Multibeam echosounders mitigate the possible aliasing problem by sampling an additional dimension. For example, low-frequency (less than a few kHz), shallow-water (i.e. propagation paths extending to tens of water depths) multibeam systems can sample in both horizontal dimensions (e.g. north and east) and time (Makris *et al.*, 2006), whereas multibeam echosounders (12–455 kHz) have been used to sample simultaneously in the vertical dimension plus one horizontal dimension and time (Brehmer *et al.*, 2006). Observation methods incorporating multibeam systems offer enhancements in several areas, including aggregation morphology-based species classification, fish avoidance from approaching vessels, more accurate biomass estimates of small schools, and an improved understanding of the relationship between fish, the environment, and anthropogenic factors (Gerlotto *et al.*, 1999; Gallaudet and De Moustier, 2002; Gerlotto and Páramo, 2003; Trenkel *et al.*, 2008). A common way to incorporate both types of systems is to use a split-beam echosounder to “calibrate” the multibeam system, such as the use of a “conventional fish finder” in the study of Makris *et al.* (2006). There are several good reasons for this type of integrated approach to investigating fish schools, including the widely

accepted, and reasonably simple, methods for calibrating split-beam systems (Foote *et al.*, 1987).

In this study, multibeam-echosounder data were combined with multifrequency, split-beam-echosounder data to provide a synoptic view of an Atlantic herring (*Clupea harengus*) school as it evolved over the course of an hour. The horizontal extent of the fish school was  $\sim 200$  m and required 1–4 minutes to traverse. Although the structure of the fish school was dynamic over this period, the data collected during each pass over the school were treated as if they were collected at a single instant in time. In essence, and to the extent that this approach is valid, this is equivalent to exchanging the time dimension for a second horizontal dimension at time-scales of less than 5 minutes. Five consecutive passes over the fish school were made, with data collected from the calibrated, split-beam and uncalibrated, multibeam echosounders. The split-beam-echosounder data were used to help classify the fish as Atlantic herring and to estimate the numerical density of fish observed directly beneath the research vessel. The multibeam echosounder was used to estimate the school volume, to describe the school morphology, and to examine the spatial heterogeneity in the packing density for each observation of the school. The spatial variability was investigated by integrating the scattering intensity along each beam, or equivalently at each beam-steering angle, for each ping. Although spatial variability was difficult to quantify in this manner because of the lack of a calibration for the multibeam echosounder as well as the unknown orientation of the fish, the method offered insights into the potential for bias when extrapolating split-beam echosounder results to an entire fish school.

## Methods

The data described here were collected as part of a larger experiment aimed at the long-range (>50 km) estimation of Atlantic herring populations on Georges Bank in the Gulf of Maine (Ratall *et al.*, 2008). The acoustic data were collected with a 400 kHz, multibeam echosounder (Reson 7125) and a multifrequency-echosounder system (Simrad EK60), equipped with 38, 120, and 200 kHz, split-beam transducers installed in the transducer well of the RV “Hugh Sharp”, at a depth of 4.0 m. The NOAA FRV “Delaware II” also participated in the experiment, by sampling pelagic fish with a high-speed, midwater, rope trawl, and collecting acoustic data with another multifrequency-echosounder system (Simrad EK500), equipped with hull-mounted, 18, 38, and 120 kHz, split-beam transducers at a depth of 3.2 m. Scheduling constraints limited the time that these two vessels could work together on the same fish aggregations, thereby restricting the amount of data collected by the RV “Hugh Sharp” that could be verified with trawl data. To mitigate this limitation, the frequency response obtained from the vessel’s multifrequency EK60 collected without the FRV “Delaware II” present was compared with the frequency response obtained from schools that were sampled with the trawl. The frequency-response data, together with the low probability of finding pelagic species other than Atlantic herring (Jech and Michaels, 2006), were used for species identification when trawls were not possible.

The three split-beam transducers on the FRV “Delaware II” were calibrated before the experiment using the standard-sphere method (Foote *et al.*, 1987). The 38 and 200 kHz, split-beam transducers on the RV “Hugh Sharp” were also calibrated using the same technique before the start of the experiment. Although the 120 kHz transducer on the RV “Hugh Sharp” was not calibrated, its response is believed to have been consistent throughout the experiment. Data associated with this transducer were used exclusively to make relative comparisons of the frequency response from aggregations, and are specific to the system used during the experiment. The Reson 7125 multibeam echosounder was not calibrated during this experiment.

During acoustic-survey operations, the EK60 on the RV “Hugh Sharp” transmitted pulses of 1024  $\mu$ s duration every second. Data were saved in the raw-file format and analysed using both the large-scale survey system post-processing software (Korneliussen *et al.*, 2006) and Matlab (The Mathworks, Inc., Natick, MA, USA). The EK500 on the FRV “Delaware II” transmitted 1024  $\mu$ s pulses at 38 and 120 kHz, and a 2056  $\mu$ s pulse at 18 kHz, and transmitted once every 2 s.

In addition to being used for estimating the frequency response, the 38 kHz EK60 data collected on the RV “Hugh Sharp” were used to derive numerical density estimates, calculated using the mean target strength ( $TS$ , dB) of the herring using the relation  $TS = 20 \log L - 71.9$ , where  $L$  corresponds to the total length of the fish (Foote, 1987). With the estimate of the mean  $TS$ , the backscattering cross section ( $\sigma_{bs}$ ) was estimated using the equation:  $\sigma_{bs} = 4 \pi 10^{(TS/10)}$ . The volume density of fish ( $\rho_v$ ) was calculated using the following formula

$$\rho_v = \frac{S_A}{\sigma_{bs}(1852)^2 \Delta z}, \quad (1)$$

where  $S_A$  is the nautical-area-scattering coefficient ( $m^2$  nautical mile $^{-2}$ ) obtained from echo integration,  $\sigma_{bs}$  the backscattering

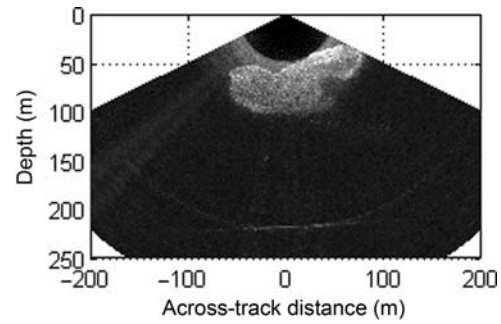


**Figure 1.** Data from a single ping of a 400 kHz, Reson 7125 multibeam echosounder. Lighter colours indicate a higher volume-backscattering strength. The seabed is faintly visible at a depth of 220 m, and the fish school appears at depths between 35 and 110 m.

cross section ( $m^2$ ), and  $\Delta z$  the difference between the upper and lower depth of the school (m).

The multibeam echosounder transmitted 300  $\mu$ s pulses once per second at maximum power. A delay of 0.5 s was used between the transmissions of the multibeam and split-beam echosounders to avoid acoustic interference. The multibeam echosounder formed 256 beams that were  $\sim 1.0^\circ$  wide in the direction of ship travel, and  $0.7^\circ$  in the athwartship direction. The full time-series for each beam was recorded using the Reson s7k data format and analysed using Matlab. An example of the multibeam-echosounder data recorded for a single ping is illustrated in Figure 1. In this image, backscatter from a fish school can be seen between depths of 35 and 100 m, as well as a weak return from the seabed at 220 m. Energy leakage into the side lobes appears wherever there is a strong return from the fish school or seabed.

For the multibeam echosounder, backscatter from fish was identified using a threshold based on local noise statistics, calculated as a function of beam and sample number. These statistics were accumulated from a 20-ping noise history before the data of interest (i.e. with no fish present). For the data in this study, the threshold was set at  $\mu_N + 2.5 \sigma_N$ , where  $\mu_N$  and  $\sigma_N$  are the mean and standard deviation (s.d.), respectively, of the noise. After thresholding the data, high backscatter corresponding to side-lobe interference was rejected by finding the maximum target amplitude at each range step and rejecting targets that were >15 dB below this maximum amplitude. Data that passed both thresholds were adjusted to a common reference by removing both the fixed and time-varying gain applied by the echosounder, applying an angularly varying gain associated with the transmit and receive beam patterns, then accounting for spreading losses, sound absorption, and resolution cell volume. These adjustments converted the raw intensity measurements into a quantity proportional to the volume-backscattering strength ( $S_v$ ). The data were then georeferenced, using the position and attitude data from an Applanix Corporation Position and Orientation System for Marine Vessels (POS/MV) installed on the RV “Hugh Sharp”, resulting in a three-dimensional set of georeferenced points whose amplitude represents  $S_v$ . To visualize the school morphology and estimate the school volume, the detected targets were converted into an evenly spaced, three-dimensional grid where the value of each grid cell is a weighted sum of the target amplitudes. The weights were calculated using a fixed-width Gaussian kernel,

which is a function of distance from the grid point. The grid was then converted into isosurfaces of constant  $S_V$ , i.e. contoured in three dimensions.

To help quantify the school morphology, six school parameters were extracted from the multibeam data. These features, which are similar to those previously reported in other studies (Nero and Magnuson, 1990; Gerlotto *et al.*, 1999; Diner, 2001), are the lateral spread, the longest horizontal distance between any two fish; school height, the longest vertical distance between any two fish; height above bottom, the vertical distance from the deepest fish to the bottom; depth below surface, the vertical distance from the shallowest fish to the surface; surface area ( $A$ ); volume ( $V$ ); and a normalized ratio of the school surface-area-to-volume ratio. The latter ratio is given in the non-dimensional form:

$$R = \frac{(A)^{1/2}}{(V)^{1/3}}. \quad (2)$$

This metric is similar to the fractal dimension used by Nero and Magnuson (1990), in that it provides an assessment of the tortuosity or fragmentation of the school, or both factors together, but avoids the implicit assumption that the school is fractal. Small values of  $R$  indicate that the school has minimized its perimeter; a sphere has an  $R = 2.2$ . Together with the  $\rho_v$  estimated from the EK60 data, and the estimated total number of fish ( $\rho_v V$ ), these variables help describe the behaviour of the school as it evolves.

## Results

Two datasets are described here. The first comprises data used to measure the frequency response of Atlantic herring collected on 26 September 2006, whereas the RV “Hugh Sharp” and the FRV “Delaware II” were conducting systematic acoustic surveys in proximity. During this time, the FRV “Delaware II” was able to sample the fish with a trawl and estimate their mean length. These data were used to verify that acoustic data collected on the RV “Hugh Sharp” when the FRV “Delaware II” was absent were probably from Atlantic herring.

The second dataset was collected after sunset on 22 September 2006. During this time, the RV “Hugh Sharp” was traversing in a southwesterly direction, generally following bathymetric contours on the northern flank of Georges Bank while collecting acoustic data and towing a GMI MKII Scanfish (a towed, undulating CTD system manufactured by EIVA in Denmark). Approximately 15 minutes after sunset, a fish school was detected, and the decision was made to recover the Scanfish and to re-acquire the fish school on the echosounder systems as often as possible to observe its evolution over time. Five passes over the fish school were made in  $\sim 1$  h, with the RV “Hugh Sharp” passing over it at speeds of 5, 4, 3, 1.5, and 2 knots for each pass. This analysis is focused on a single school that was simultaneously observed on the multibeam and split-beam echosounders. Several other similar schools of Atlantic herring were thought to have been in this area at the same time, based on the multibeam-echosounder observations, and also on the low-frequency (nominally 1 kHz) Ocean Acoustic Waveguide Remote Sensing system (Makris *et al.*, 2006) that was operating in the area (P. Ratilal, pers. comm.).

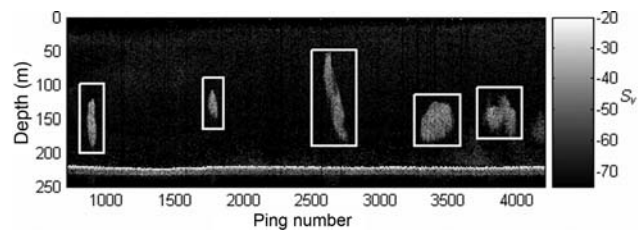


**Figure 2.** Volume-backscattering strength data from the 38 kHz EK60 illustrating five consecutive passes over the same school (outlined) imaged on both the single-beam and multibeam echosounders.

## Observed frequency response and species identification

The relative frequency response generated from the EK500 data collected on the FRV “Delaware II” during 26 September decreased in  $S_V$  from lower to higher frequencies, with a stronger decrease evident from 18 to 38 kHz than between 38 and 120 kHz. The 18 and 120 kHz  $S_V$  were 2.4 times higher and 1.1 times lower than the 38 kHz  $S_V$ , respectively, when averaged over 11 separate schools. Trawling in this area confirmed that the  $S_V$  frequency response represented Atlantic herring. These results were similar to those obtained by Fernandes *et al.* (2006), who compiled available information on multifrequency data for commercial species. The relative frequency response generated from the EK60 data collected on the RV “Hugh Sharp”, surveying in the same area on 26 September, decreased in backscattering strength from 38 to 200 kHz, but increased between 38 and 120 kHz. The 120 and 200 kHz  $S_V$  data were 1.8 times higher and 1.4 times lower than the 38 kHz  $S_V$ , respectively, when averaged over seven separate schools. Because only the 38 and 200 kHz transducers were calibrated during this experiment, the frequency response from the RV “Hugh Sharp” was only used to help classify fish schools observed when no trawling was done.

On 22 September 2006, data were recorded from both the EK60 and the Reson 7125 on the RV “Hugh Sharp” as it made multiple passes over a single school of fish (Figure 2). The relative EK60 frequency response for each of the five passes was similar to the frequency-response data for 26 September. On average, the 120 and 200 kHz  $S_V$  data were 1.5 times higher and 2.0 times lower than the 38 kHz  $S_V$ , respectively, indicating that the data represented Atlantic herring.

## Observations of a single school over time

Although the morphological evolution of the fish school imaged on 22 September is difficult to ascertain completely from the 38-kHz EK60 data (Figure 2), the school morphology clearly changed on each pass as the fish appeared initially to rise in the water column, then spread vertically, and then return to deeper water as a lower density school, possibly fragmenting on the final pass. In addition to these qualitative observations, the 38 kHz EK60 data were used to generate estimates of the fish density using Equation (1). Because this school was not trawled, the mean  $L$  of Atlantic herring (26 cm) collected on board the FRV “Delaware II” during the experiment was used for this calculation. For the five passes over the fish school, fish density was highest during the initial pass at  $1.10 \text{ fish m}^{-3}$  (Figure 3), probably representing the fish in their undisturbed state (i.e. before the ship had passed over them and the Scanfish had possibly been towed

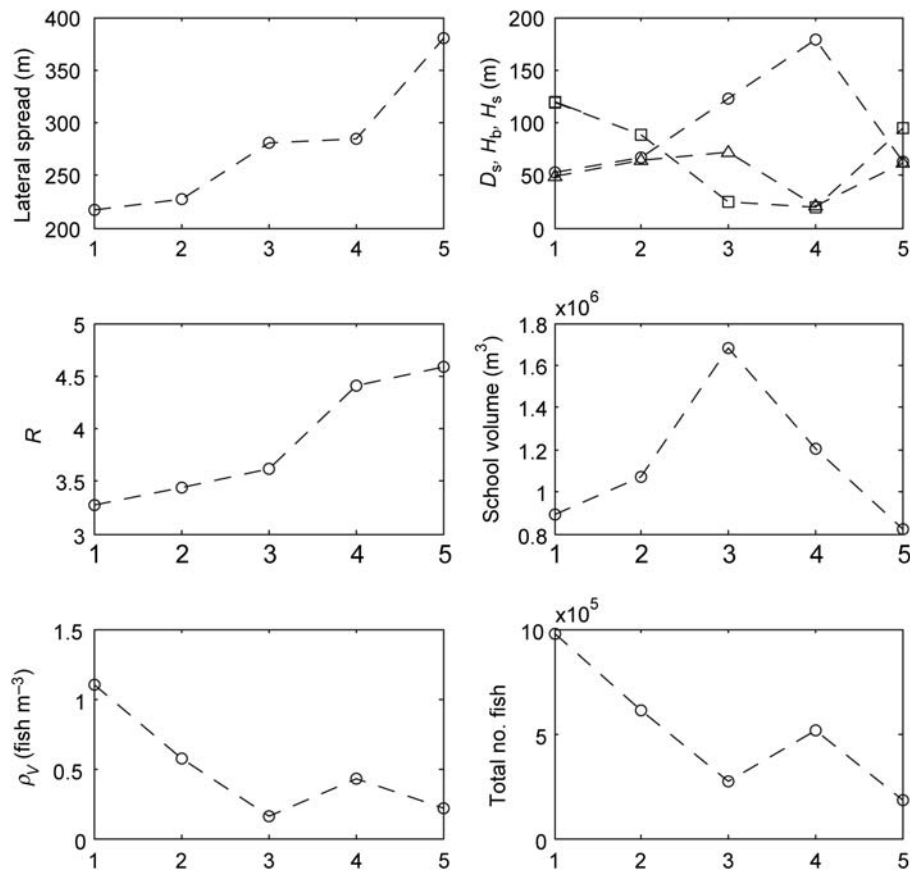


**Figure 3.** School parameters extracted from the multibeam and single-beam echosounders corresponding to each of the five passes. In the upper-right panel,  $D_s$  is the depth below surface (squares),  $H_b$  is the height above bottom (triangles), and  $H_s$  is the school height (circles). In the middle and lower-left panels,  $R$  is the normalized ratio of the school surface-area-to-volume ratio and  $\rho_v$  is the fish-number density.

through them). Fish-density estimates decreased in each subsequent pass.

The multibeam-echosounder data were used to highlight further changes in school morphology over the five passes, as well as to calculate the school volume. The school images identified in Figure 2 are shown in Figures 4 and 5. These school images are displayed in a fixed, relative coordinate system, i.e. the position 0, 0, 0 represents the same point on the earth for each of the five images. The plan view used in Figure 4 indicates that, on average, the fish moved latterly only a few hundred metres during the time in which the five school images were acquired. There were, however, significant changes in school depth and general morphology (Figure 3). After the first pass, the school began to expand, almost doubling its volume by the third pass while both the lateral spread and height of the school increased. Over the first three passes, the increase in school height was dominated by a rapid rise of some of the fish towards the surface. On the third pass, fish were detected as shallow as 25 m and as deep as 140 m, although it should be noted that the shallowest portion of the school extended to the edge of the multibeam field of view, and, presumably, outside it, where the fish may have been shallower. Hence, the school volume on the third pass may have been biased low. During these first three passes, the school volume steadily increased and the fish-number density decreased, indicating a dilation of the school. After the third pass,  $R$  jumped to its highest level as the

school began to exhibit fragmentation. Note the assumption that the fragments visible in the fourth and fifth passes (Figures 4 and 5) were considered members of the original school. This is reflected in the school metrics in Figure 3.

One of the limitations of combining the single-beam and multibeam data in this way becomes apparent when both the  $\rho_v$  and the  $V$  are combined to estimate the total number of fish. If the  $\rho_v$  observed by the split-beam echosounder is taken to be representative of the entire school then, except the fourth pass, the total number of fish decreases throughout the five passes. School fragmentation and escapement outside the multibeam field of view could have caused the estimates of  $V$  to be biased low. However, it is also quite likely that density was heterogeneous within the school, causing the split-beam data to introduce significant bias in estimates of fish density. Although the multibeam data, complicated by lack of knowledge of the orientation of the fish, were not considered calibrated to the accuracy of the EK60, it is nevertheless possible to investigate this limitation. To do this, the fish-school returns from the multibeam were averaged along each beam for each ping. This procedure resulted in images that represent the beam-averaged scattering intensity as a function of beam-steering angle (Figure 6). If the fish were uniformly distributed throughout the school, which is the underlying assumption when estimating total fish number, and the fish maintained no preferential orientation, the angular dependence of the scattering intensity should appear the same for each school



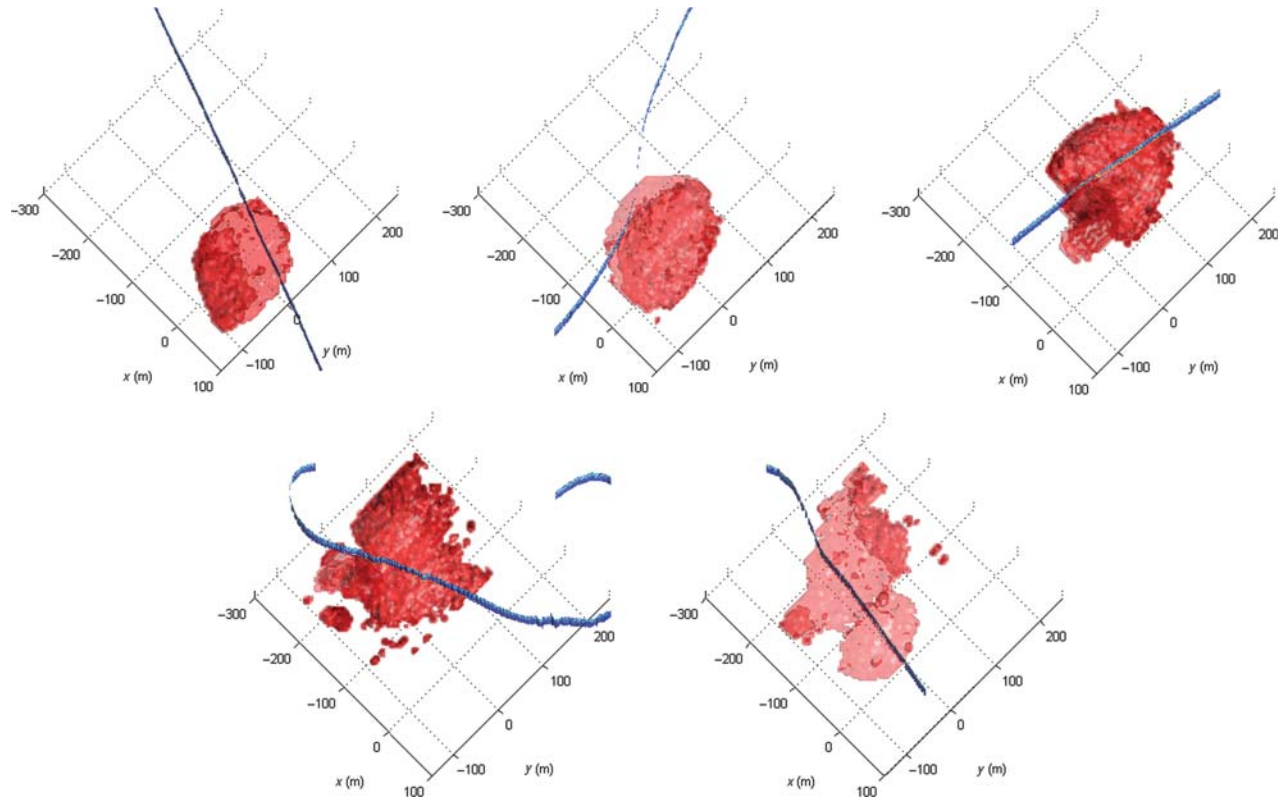


**Figure 4.** A plan view of the school morphology on five consecutive passes (clockwise, from upper left). The red surfaces are derived from the Reson 7125 data. The blue line is derived from the 38 kHz, EK60 data and indicates the track of the vessel.

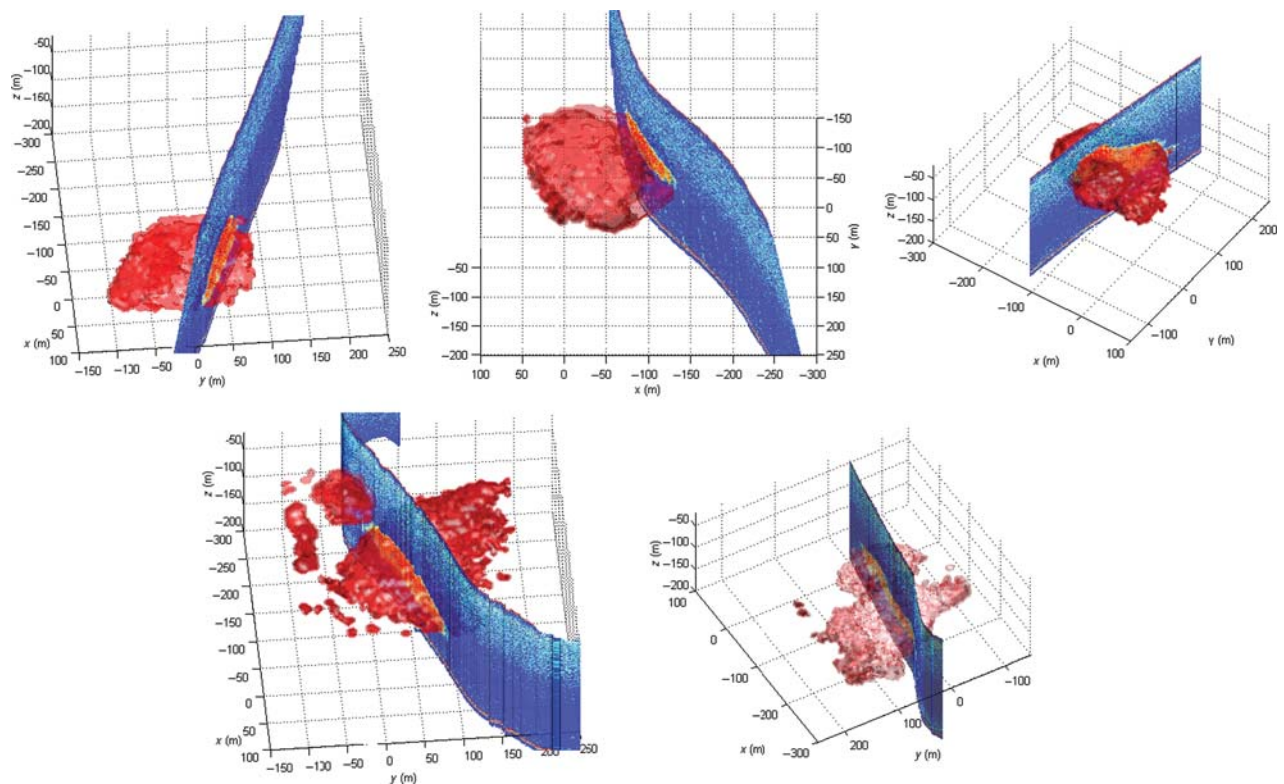


**Figure 5.** The same data as those displayed in Figure 4, but displayed from an oblique angle.

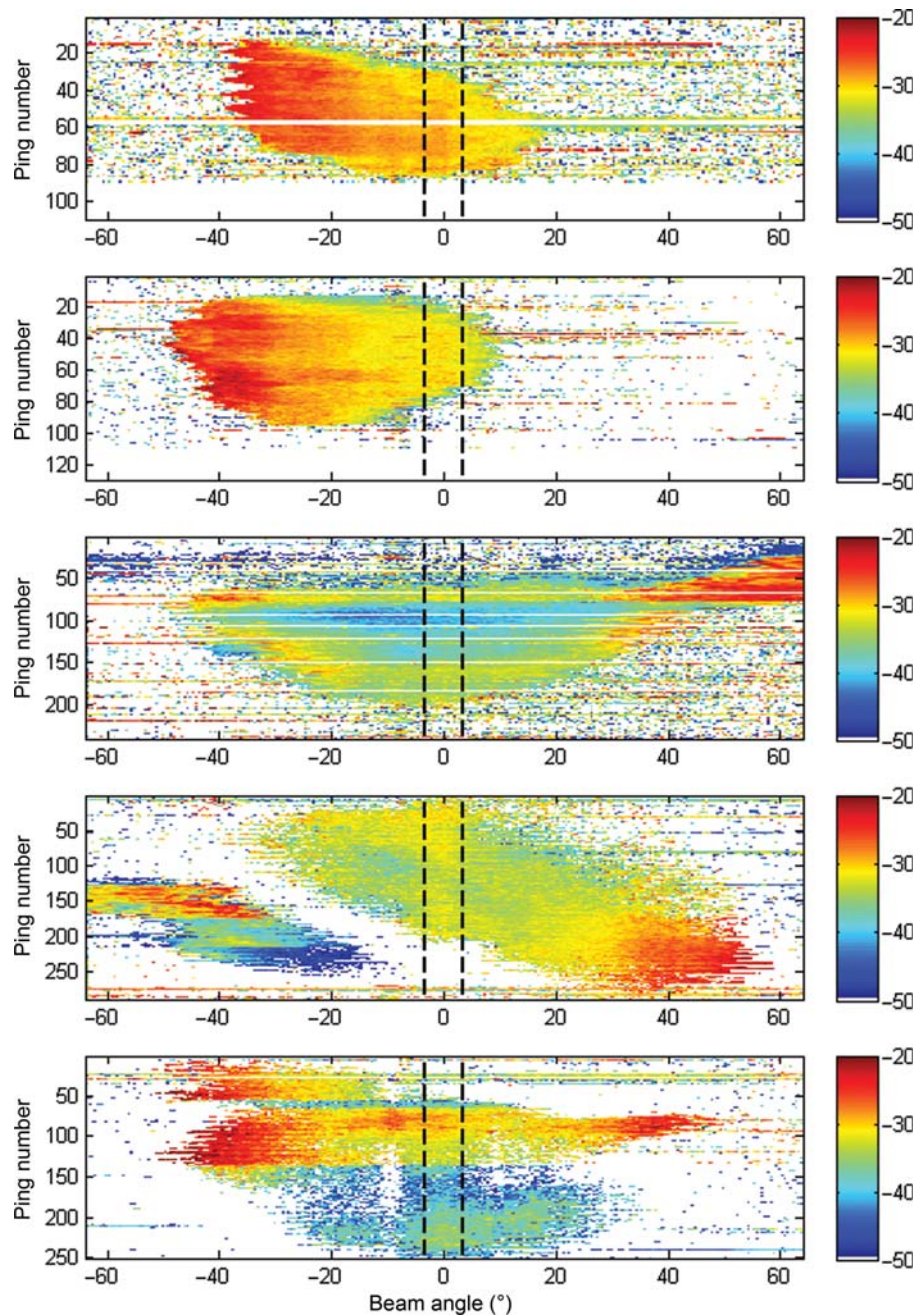


**Figure 6.** The beam-averaged scattering intensity observed with the multibeam echosounder for each of the five passes, in order, from top to bottom. The black dashed lines indicate the nominal field of view for the EK60. Lighter colours (in dB, arbitrary units) indicate a higher scattering strength.

image. That is, the relative difference in intensity between any pair of beam angles should be the same on each pass. The data in Figure 6 indicate that this was not the case. If the fish are assumed nominally uniformly distributed on the first pass, they revealed higher densities on the port side on the second pass and a more complicated non-uniformity on the third, fourth, and fifth passes. The split-beam echosounder field of view is confined to  $\pm 3.5^\circ$ , as indicated by the dashed lines in Figure 6. With higher densities outside this field of view, it appears that the fish density was potentially underestimated on each pass after the first.

Similar disparity in the angular dependence of the scattering intensity between passes can be a result of a preferential orientation of the fish (Cutter and Demer, 2007). For example, we might expect to see a greater variation in scattering intensity with angle when the fish are orientated across the ship's track (dorsal view on the centre beam and near-head/tail view on the outermost beam) than when the fish were orientated in the along-track direction (Jech and Horne, 2002; Towler *et al.*, 2003). If this were the case here, a comparison of the first two passes in Figure 6 indicates that the fish would have been orientated more along the track line of the ship (Figure 4) on the first pass over the school



than on the second. Alternatively, perhaps the fish tilt increased after the first pass, causing a decrease in the scattering intensity below the ship (near  $0^\circ$ ) relative to the outer beams. In fact, both scenarios could have been true. The school images in Figure 4 indicate that the school had moved at  $\sim 6 \text{ cm s}^{-1}$  in the direction of the track line corresponding to the first pass of the ship, and the vertical school parameters, depth below surface and height above bottom, indicate that the fish had risen in the water column after the first pass. Although this increases the likelihood that fish orientation was playing a role in the angular-dependent backscatter illustrated in Figure 6, it does not explain the asymmetry in scattering intensity across beam angles that was apparent on any given ping. This asymmetry is especially evident in Figure 6 for pings 50–70 on the first pass, pings 35–65 on the second pass, and pings 130–170 on the third pass, where in each case the angular dependence for negative beam angles did not match that for positive beam angles. This indicates that a spatially varying fish density remained present, regardless of the possible orientation of the fish.

## Discussion

The observations described here illustrate some of the advantages of combining data from multifrequency, split-beam and multi-beam echosounders. In addition to providing multifrequency data that can be used to aid species classification, the more easily calibrated, split-beam echosounder provides a quantitative estimate of the fish-number density directly beneath the vessel. Information from the multibeam echosounder complements this type of data with estimates of school volume, synoptic views of the entire school, and location within the water column. For small schools (i.e. those that can be entirely imaged by the multi-beam echosounder), combining these two measurements improves both estimates of the number of fish and assessments of fish behaviour.

Limitations of this approach remain apparent, particularly when considering that the density of fish within a school may often exhibit spatial inhomogeneities (Misund, 1993; Fréon and Misund, 1998). In this study, the simple approach of extrapolating the estimates of fish density measured directly beneath the vessel to the entire fish school appears to have resulted in a fish count that was biased low, at least after the initial pass over the school. This potential bias was explored by examining the angular dependence in the beam-integrated scattering strength over the five passes. This angular dependence could have been caused by a combination of spatial inhomogeneity in the fish-number density and by changes in the orientation of the fish with respect to the multibeam echosounder, as explored by Cutter and Demer (2007).

It is a non-trivial task to remove these biases in the fish count. The multibeam echosounder must be calibrated, the acoustic-scattering properties of the fish must be known across all incidence angles at the multibeam frequency (Jech and Horne, 2002; Towler *et al.*, 2003; Okumura and Masuya, 2004; Reeder *et al.*, 2004), and knowledge of the orientation of the fish relative to the multibeam is required. Although calibrating multibeam echosounders is not done as readily as split-beam echosounders, it is certainly possible and it has been done by several other investigators (Cochrane *et al.*, 2003; Melvin *et al.*, 2003; Foote *et al.*, 2005). New approaches to fishery multibeam echosounders may make *in situ* calibrations more feasible (Trenkel *et al.*, 2008). The orientation of the fish may be the most challenging aspect of quantifying multibeam output to estimate fish abundance. For

repeat passes, the motion of the school may be determined and used to estimate an average orientation. In this study, the school moved only a few hundred metres during an hour, so we expect that they had a uniform (over  $360^\circ$ ) distribution in azimuth. Such estimates of orientation would be complicated, however, if strong currents are present, or when only one pass over the school is possible.

## Acknowledgements

The authors thank Nicholas Makris (Massachusetts Institute of Technology) and Purnima Ratilal (Northeastern University) for the invitation to participate in this work. We also thank Richard Menis (Naval Research Laboratory), who was the chief scientist on RV “Hugh Sharp”, Ruben Patel (Institute of Marine Research), and the captains, crews, and scientific teams aboard the RV “Hugh Sharp” and the NOAA FRV “Delaware II”, for their assistance during these experiments. We are also grateful to Chris Malzone (Reson) for the use of the Reson 7125, Kelly Benoit-Bird (Oregon State University) for the use of her EK60 transducers, and Rick Towler (Alaska Fisheries Science Center, NOAA) for his Matlab code.

## References

- Brehmer, P., Lafont, T., Georgakarakos, S., Josse, E., Gerlotto, F., and Collet, C. 2006. Omnidirectional multibeam sonar monitoring: applications in fisheries science. *Fish and Fisheries*, 7: 165–179.
- Cochrane, N. A., Li, Y., and Melvin, G. D. 2003. Quantification of a multibeam sonar for fisheries assessment applications. *Journal of the Acoustical Society of America*, 114: 745–758.
- Cutter, G. R., and Demer, D. A. 2007. Accounting for scattering directivity and fish behaviour in multibeam-echosounder surveys. *ICES Journal of Marine Science*, 64: 1664–1674.
- Diner, N. 2001. Correction on school geometry and density: approach based on acoustic image simulation. *Aquatic Living Resources*, 14: 211–222.
- Fernandes, P. G., Korneliussen, R. J., Lebourges-Dhaussy, A., Masse, J., Iglesias, M., Diner, N., Ona, E., *et al.* 2006. The SIMFAMI project: species identification methods from acoustic multifrequency information. Final Report to the EC Q5RS-2001-02054. FRS Marine Laboratory Aberdeen, Aberdeen, UK. 500 pp.
- Foote, K. G. 1987. Fish target strength for use in echo integrator surveys. *Journal of the Acoustical Society of America*, 82: 981–987.
- Foote, K. G., Chu, D., Hammar, T. R., Baldwin, K. C., Mayer, L. A., Hufnagle, L. C., and Jech, J. M. 2005. Protocols for calibrating multibeam sonar. *Journal of the Acoustical Society of America*, 117: 2013–2027.
- Foote, K. G., Knudsen, H. P., Vestnes, G., MacLennan, D. N., and Simmonds, E. J. 1987. Calibration of acoustic instruments for fish density estimation: a practical guide. ICES Cooperative Research Report, 144. 69 pp.
- Fréon, P., and Misund, O. A. 1998. Dynamics of Pelagic Fish: Distribution and Behaviour: Effects on Fisheries and Stock Assessment. Fishing News Books, Oxford. 348 pp.
- Gallaudet, T. C., and De Moustier, C. P. 2002. Multibeam volume acoustic backscatter imagery and reverberation measurements in the northeastern Gulf of Mexico. *Journal of the Acoustical Society of America*, 112: 489–503.
- Gerlotto, F., and Páramo, J. 2003. The three-dimensional morphology and internal structure of clupeid schools as observed using vertical scanning multibeam sonar. *Aquatic Living Resources*, 16: 113–122.
- Gerlotto, F., Soria, M., and Fréon, P. 1999. From two dimensions to three: the use of multibeam sonar for a new approach in fisheries acoustics. *Canadian Journal of Fisheries and Aquatic Sciences*, 56: 6–12.

- Jech, J. M., and Horne, J. K. 2002. Three-dimensional visualization of fish morphometry and acoustic backscatter. *Acoustic Research Letters Online*, 3: 35–40. [ojps.aip.org/ARLO](http://ojps.aip.org/ARLO).
- Jech, J. M., and Michaels, W. L. 2006. A multifrequency method to classify and evaluate fisheries acoustics data. *Canadian Journal of Fisheries and Aquatic Sciences*, 63: 2225–2235.
- Korneliussen, R. J., Ona, E., Eliassen, I., Heggelund, Y., Patel, R., Godø, O. R., Giertsen, C., *et al.* 2006. The Large Scale Survey System - LSSS. *Proceedings of the 29th Scandinavian Symposium on Physical Acoustics*, Ustaoset, 29 January – 1 February 2006. 6 pp. ISBN 82-8123-001-0.
- Makris, N. C., Ratilal, P., Symonds, D. T., Jagannathan, S., Lee, S., and Nero, R. W. 2006. Fish population and behavior revealed by instantaneous continental shelf-scale imaging. *Science*, 311: 660–663.
- Melvin, G. D., Cochrane, N. A., and Li, Y. 2003. Extraction and comparison of acoustic backscatter from a calibrated multi- and single-beam sonar. *ICES Journal of Marine Science*, 60: 669–677.
- Misund, O. A. 1993. Dynamics of moving masses: variability in packing density, shape, and size among herring, sprat, and saithe schools. *ICES Journal of Marine Science*, 50: 145–160.
- Nero, R. W., and Magnuson, J. J. 1990. Characterization of patches along transects using high-resolution 70 kHz integrated acoustic data. *Canadian Journal of Fisheries and Aquatic Sciences*, 46: 2056–2064.
- Okumura, T., and Masuya, T. 2004. Three dimensional morphometry of fish body structure by X-ray CT. *Oceans 2004*, 1: 354–356.
- Ratilal, P., Gong, Z., Cocuzzo, D., Andrews, M., Jagannathan, S., Bertsatos, I., Chen, T., *et al.* 2008. Spawning behaviour and spatial distribution of Atlantic herring on Georges Bank revealed by ocean acoustics waveguide remote sensing. *Journal of the Acoustical Society of America*, 123: 3103.
- Reeder, D. B., Jech, J. M., and Stanton, T. K. 2004. Broadband acoustic backscatter and high-resolution morphology of fish: measurements and modelling. *Journal of the Acoustical Society of America*, 116: 747–761.
- Simmonds, J., and MacLennan, D. N. 2005. *Fisheries Acoustics: Theory and Practice*, 2nd edn. Blackwell Science, Oxford, UK. 437 pp.
- Towler, R. H., Jech, J. M., and Horne, J. K. 2003. Visualizing fish movement, behaviour, and acoustic backscatter. *Aquatic Living Resources*, 16: 277–282.
- Trenkel, V. M., Mazauric, V., and Berger, L. 2008. The new fisheries multibeam echosounder ME70: description and expected contribution to fisheries research. *ICES Journal of Marine Science*, 65: 645–655.

doi:10.1093/icesjms/fsp090